Supporting Information for

Original article

Autophagy enhanced by curcumin ameliorates inflammation in atherogenesis *via* the TFEB–p300–BRD4 axis

Xuesong Li[a,†], Ruigong Zhu[a,†], Hong Jiang[a,†], Quanwen Yin[a], Jiaming Gu[a], Jiajing Chen[a], Xian Ji[a], Xuan Wu[a], Haiping Fu[a], Hui Wang[a], Xin Tang[a], Yuanqing Gao[a], Bingjian Wang[d,*], Yong Ji[a,b,*], Hongshan Chen[a,b,c,d,*]

[a]*Key Laboratory of Cardiovascular and Cerebrovascular Medicine, School of Pharmacy, Nanjing Medical University, Nanjing 211166, China*

[b]*Key Laboratory of Targeted Intervention of Cardiovascular Disease, Collaborative Innovation Center for Cardiovascular Disease Translational Medicine, Nanjing Medical University, Nanjing 211166, China*

[c]*Department of Cardiothoracic Surgery, the Second Affiliated Hospital of Nanjing Medical University, Nanjing 211166, China*

[d]*Department of Cardiology, Huai'an First People's Hospital Affiliated with Nanjing Medical University, Huai'an 223399, China*

Received 4 September 2021; 13 November 2021; accepted 17 November 2021

[†]These authors made equal contributions to this work.

[*]Corresponding authors. Tel.: +86 025 86868467.

E-mail addresses: hongshanchen@njmu.edu.cn (Hongshan Chen), yongji@njmu.edu.cn (Yong Ji), hayywbj@njmu.edu.cn (Bingjian Wang).

Supporting tables

Table S1 The sequence of siRNAs used in this study.

Gene name	No.	5′→3′	5′→3′
BRD4	1	GCGUUUCCACGGUACCAAATT	UUUGGUACCGUGGAAACGCTT
	2	GGAAACCUCAAGCUGAGAATT	UUCUCAGCUUGAGGUUUCCTT
	3	CCGUGAUGCUCAGGAGUUUTT	AAACUCCUGAGCAUCACGGTT
ATG5	1	GGACGAAUUCCAACUUGUUTT	AACAAGUUGGAAUUCGUCCTT
	2	CCAUCAAUCGGAAACUCAUTT	AUGAGUUUCCGAUUGAUGGTT
	3	GGAAGCAGAACCAUACUAUTT	AUAGUAUGGUUCUGCUUCCTT
TFEB	1	GGCUACAUCAAUCCUGAAATT	UUUCAGGAUUGAUGUAGCCTT
	2	GACGAAGGUUCAACAUCAATT	UUGAUGUUGAACCUUCGUCTT
	3	CAGGCUGUCAUGCAUUACATT	UGUAAUGCAUGACAGCCUGTT

Table S2 Antibodies used in this study.

Factor or PTM	Vendor	Cat. No.	Dilution for blotting	Vol. for ChIP (μL)
P62	Cell Signaling Technology	5114S	1:1,000	
LC3	Proteintech	14600-1-AP	1:1,000	
Actin	Biogot	AP0060	1:1,000	
TFEB	Santa	sc-166736	1:1,000	10
TFEB	Proteintech	13372-1-AP	1:1,000	
p-TFEB	Affinity	AF3708	1:1,000	
PCNA	Cell Signaling Technology	13110	1:1,000	
ATG5	Cell Signaling Technology	12994	1:1,000	
P300	Abcam	ab54984	1:1,000	
P300	Bethyl	A300-358A		10
BRD2	Santa	sc-393720	1:1,000	
BRD2	Cell Signaling Technology	5848S		10
BRD3	Proteintech	11859-1-AP	1:1,000	8
BRD4	Abcam	ab243862	1:1,000	10
Histone 3	Abcam	ab1791	1:1,000	8
mTOR	Cell Signaling Technology	2972S	1:1,000	
p-mTOR	Cell Signaling Technology	2971S	1:1,000	
Acetylated histone 3	Abcam	ab4729	1:1,000	
MED1	Bethyl	A300-793A	1:1,000	5
AKT	Cell Signaling Technology	9272	1:1,000	
p-AKT	Cell Signaling Technology	4060S	1:1,000	
Calcineurin	Cell Signaling Technology	2614	1:1,000	
S6K1	Cell Signaling Technology	34475	1:1,000	
p-S6K1	Cell Signaling Technology	97596	1:1,000	
H3K27ac	Abcam	ab177178	1:1,000	8
H3K4me1	Abcam	ab176877	1:1,000	
H3K27me3	Abcam	ab6002	1:1,000	
H3K9ac	Abcam	ab32129	1:1,000	
H3K14ac	Abcam	ab52946	1:1,000	
H3K18ac	Abcam	ab177870	1:1,000	
H3K23ac	Abcam	ab177275	1:1,000	
BTK	Proteintech	21581-1-AP	1:1,000	
p-BTK	Cell Signaling Technology	5082	1:1,000	
HRP-conjugated goat anti-rabbit secondary antibody	Jackson Labs	111035003	1:30,000	
HRP-conjugated goat anti-mouse secondary antibody	Jackson Labs	115036003	1:30,000	

Table S3 RT-PCR primers used in this study.

Gene name	Forward sequence	Reverse sequence
TFEB	CCGGATGTAATCCACAGAGGC	AAGGAGCGGCAGAAGAAAGAC
ATG5	GCTGTGATGAAGAAAGTGTGGTAAA	AATGAATGAGGAAGTAAAAATGGGC
BRD4	CACATCCACCAGAAACCAG	AGCGAAGACTCCGAAACA
IL-6	CCTCCAGAACAGATTTGAGAGTAGT	GGGTCAGGGGTGGTTATTGC
TNF-α	AGGACACCATGAGCACTGAAAGC	AAGGAGAAGAGGCTGAGGAACAAG
IL-1β	GAAATGATGGCTTATTACAGTGGCA	GTAGTGGTGGTCGGAGATTCGTAG
MCP-1	TAGCAGCCACCTTCATTC	CTTCTTTGGGACACTTGCT
IL-8	GACATACTCCAAACCTTTCCACCC	TTCAAAAACTTCTCCACAACCCTC
Actin	CTACCTCATGAAGATCCTCACCGA	TTCTCCTTAATGTCACGCACGATT

Table S4 ChIP primers used in this study.

Primer set name	Forward sequence	Reverse sequence
IL-1β-(–)1 kb	AACCGAGACACCAGCAAAGT	GCAGACCTGTCAAAGAGGCA
IL-1β-P	GAATCCCAGAGCAGCCTGTT	AACAGCGAGGGAGAAACTGG
IL-1β-(+)1 kb	CTACTCCTCCCCTGTCACCA	TTCCAGTGAGACACAGGCTG
IL-6-(–)1 kb	GGCACAGAGAGCAAAGTCCT	CACCTGCTTCAGCCCACTTA
IL-6-P	CACCCTCACCCTCCAACAAA	TTCTCTTTCGTTCCCGGTGG
IL-6-(+)1 kb	GGGTCTGAAATCCATGCCCA	CTAGTCCTTCCAAAGCCCGG
TNF-α-(–)1 kb (TNF, TNFA)	TCCAGGGCTATGGAAGTCGA	GGTCCTGGAGGCTCTTTCAC
TNF-α-P (TNF, TNFA)	TGCTTGTGTGTCCCCAACTT	CTGCACCTTCTGTCTCGGTT
TNF-α-(+)1 kb (TNF, TNFA)	CCTTCTCCCCAACAGTTCCC	ACCGGTACTAACCCTACCCC
MCP-1-(–)1 kb (CCL2)	ACTGCTGCCTGCTATGCTAG	TTCCAAATGGGCAGACAGCT
MCP-1-P (CCL2)	TCTCGCCTCCAGCATGAAAG	CTTGGGGAATGAAGGTGGCT
MCP-1-(+)1 kb (CCL2)	GAGCAAGGGACAAGCCTCAT	GGTGGAGAGTGATGTTGGGG
IL-8-(–)1 kb (CXCL8)	CCCTCCACAGTGTGTTCACA	TTCGCTTCTGGGCAAGTACA
IL-8-P (CXCL8)	CAGAGACAGCAGAGCACACA	CCTTCACACAGAGCTGCAGA
IL-8-(+)1 kb (CXCL8)	CCCCAACAGGTGCAGTTTTG	TGGGGTGGAAAGGTTTGGAG

Supporting figures

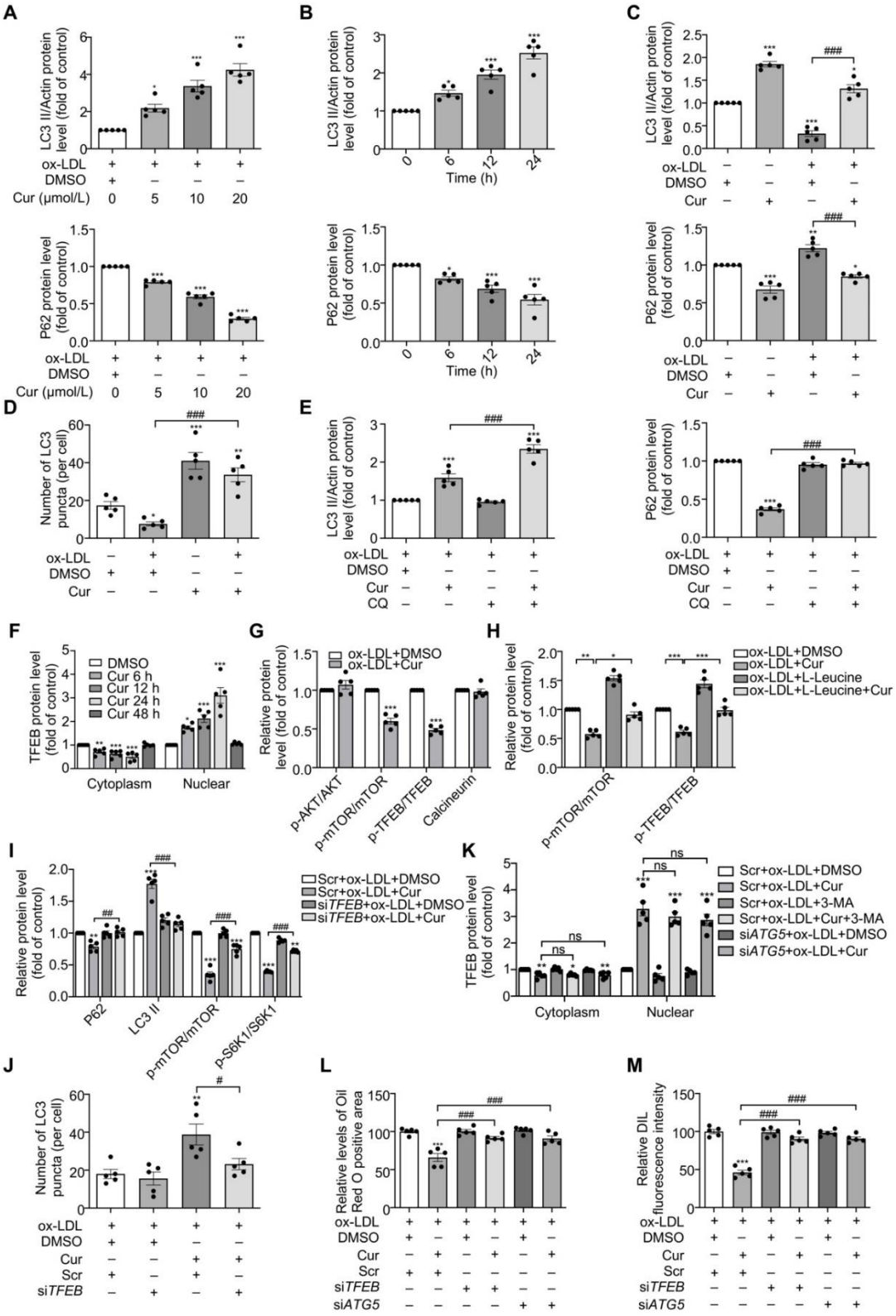

Figure S1 The statistical graphs of the results in Fig. 1. (A–C) The bar graph of immunoblot analysis of endogenous LC3 II and P62 in foam cells (FCs) treated as in Fig. 1C (A), Fig. 1D (B), Fig. 1E (C). (D) The bar graph of the immunofluorescence staining of LC3 in oxidized low-density lipoprotein (ox-LDL)-treated macrophages challenged with Cur in Fig. 1F. (E) The bar graph of immunoblot analysis of autophagic flux in FCs treated as in Fig. 1G. (F) The bar graph of immunoblot analysis of TFEB subcellular distribution in FCs treated as in Fig. 1H. (G) The bar graph of immunoblot analysis of mTOR/p-mTOR, AKT/p-AKT, calcineurin and TFEB/p-TFEB in FCs treated as in Fig. 1I. (H) The bar graph of immunoblot analysis of the effect of mTORC1 specific agonist L-leucine on the activity of mTOR and TFEB as treated in Fig. 1J. (I) The bar graph of immunoblot analysis of autophagy-related proteins in FCs as treated in Fig. 1K. (J) The bar graph of immunofluorescence analysis of LC3 (green) in FCs as treated in Fig. 1L. (K) The bar graph of immunoblot analysis of the subcellular distribution of TFEB in FCs as treated in Fig. 1M. (L, M) The bar graph of Oil red O staining (ORO) in Fig. 1O (L) and 1,1′-dioctadecyl-3,3,3′,3′-tetramethy-lindocarbocyanine perchlorate labeled oxidized low-density lipoprotein (Dil-ox-LDL) analysis in Fig. 1P (M) in Cur-treated FCs combined with si*TFEB* or si*ATG5*. Data are expressed as mean ± SEM, $n = 5$. $^{*}P < 0.05$, $^{**}P < 0.01$, $^{***}P < 0.001$; $^{\#}P < 0.05$, $^{\#\#}P < 0.01$, $^{\#\#\#}P < 0.001$; ns, no significance.

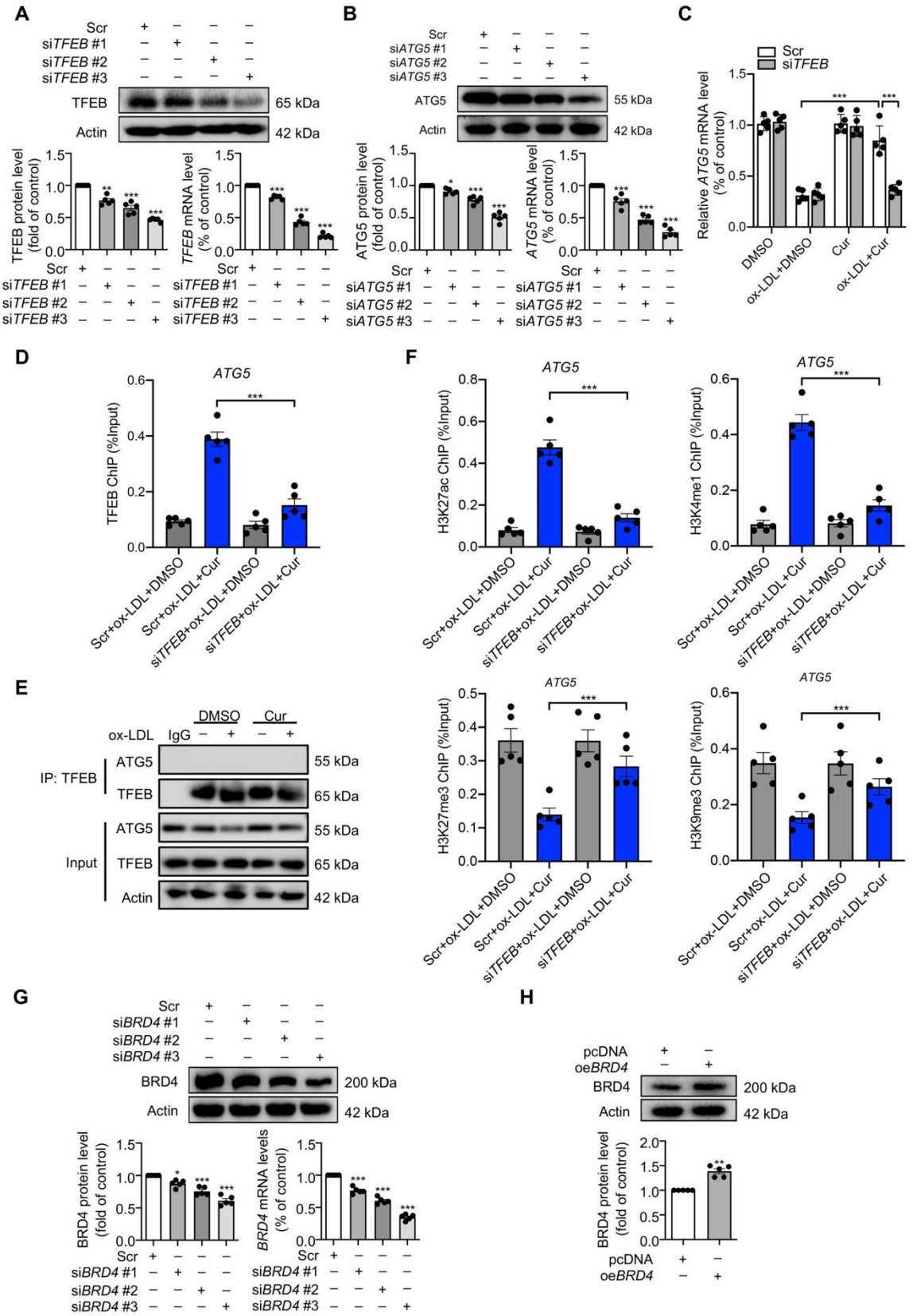
A
Scr
siTFEB #1
siTFEB #2
siTFEB #3
TFEB
65 kDa
Actin
42 kDa
TFEB protein level (fold of control)
TFEB mRNA level (% of control)
B
siATG5 #1
siATG5 #2
siATG5 #3
ATG5
55 kDa
ATG5 protein level (fold of control)
ATG5 mRNA level (% of control)
C
Scr
siTFEB
Relative ATG5 mRNA level (% of control)
DMSO
ox-LDL+DMSO
Cur
ox-LDL+Cur
D
ATG5
TFEB ChIP (%Input)
Scr+ox-LDL+DMSO
Scr+ox-LDL+Cur
siTFEB+ox-LDL+DMSO
siTFEB+ox-LDL+Cur
F
H3K27ac ChIP (%Input)
H3K4me1 ChIP (%Input)
H3K27me3 ChIP (%Input)
H3K9me3 ChIP (%Input)
E
ox-LDL
IgG
IP: TFEB
Input
G
siBRD4 #1
siBRD4 #2
siBRD4 #3
BRD4
200 kDa
BRD4 protein level (fold of control)
BRD4 mRNA levels (% of control)
H
pcDNA
oeBRD4

Figure S2 The interference and overexpression efficiency of proteins, and the interaction between TFEB and ATG5 in FCs treated with Cur. (A, B) Immunoblot and qRT-PCR analysis of interference efficiency targeting *TFEB* (A) and *ATG5* (B) in macrophages. (C) qRT-PCR analysis of the mRNA level of *ATG5* in ox-LDL-treated macrophages in the presence of si*TFEB*. (D) Chromatin immunoprecipitation (ChIP) analysis of the enrichment of TFEB at the promoter of *ATG5* in Cur-treated FCs combined with si*TFEB*. (E) Co-immunoprecipitation analysis of the protein interaction between TFEB and ATG5 in macrophages treated with ox-LDL in the presence of Cur. (F) ChIP analysis of the enrichment of H3K4me1, H3K9me3, H3K27ac and H3K27me3 at the promoter region of *ATG5* in FCs treated with Cur in the presence of si*TFEB*. (G) Immunoblot and qRT-PCR analysis of interference efficiency targeting *BRD4* in macrophages. (H) Immunoblot analysis of the overexpression efficiency targeting BRD4 in macrophages. Data are expressed as mean ± SEM, $n = 5$. $^{*}P < 0.05$, $^{**}P < 0.01$, $^{***}P < 0.001$.

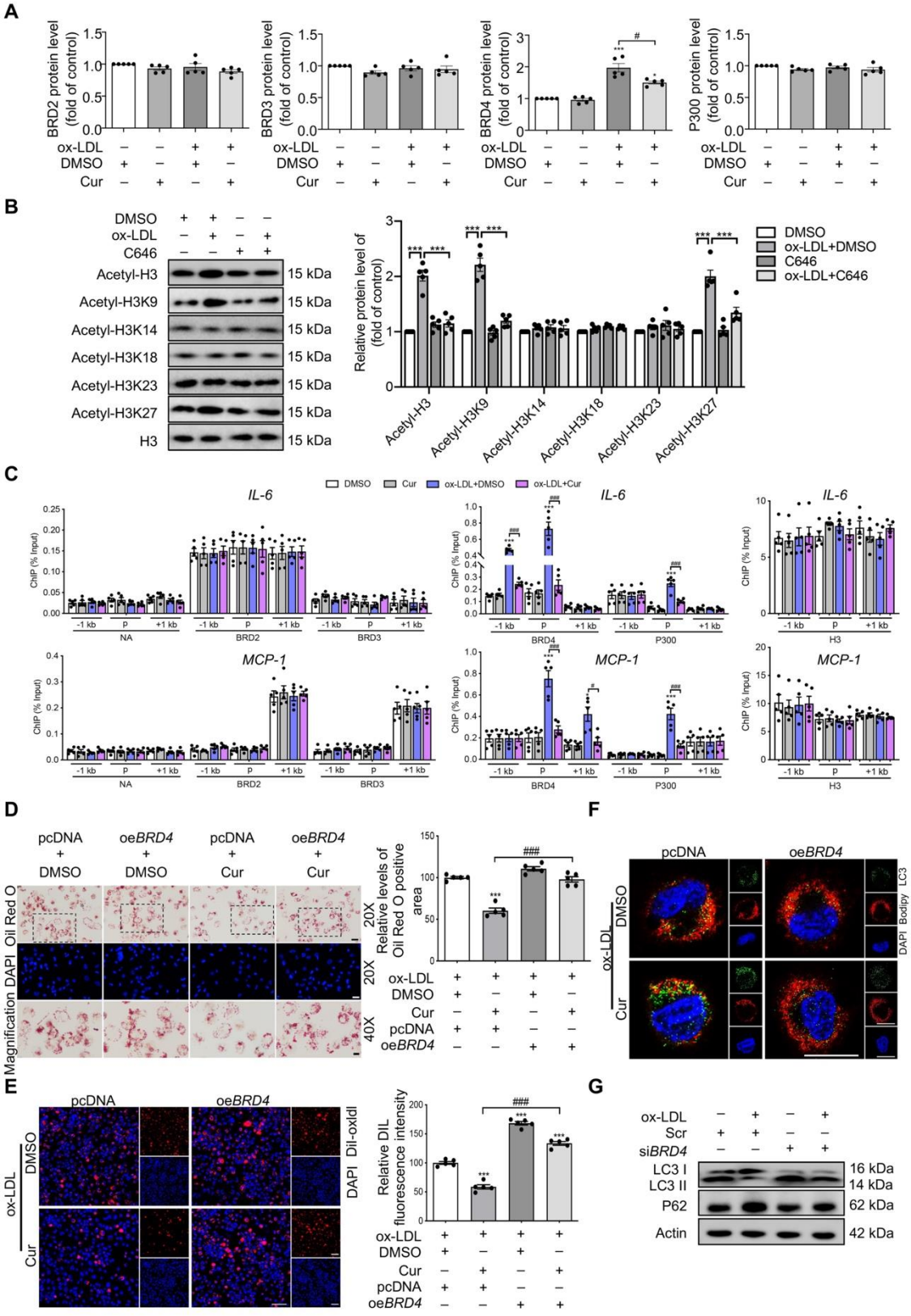
A
BRD2 protein level (fold of control)
BRD3 protein level (fold of control)
BRD4 protein level (fold of control)
P300 protein level (fold of control)
ox-LDL
DMSO
Cur
B
DMSO
ox-LDL
C646
Acetyl-H3
Acetyl-H3K9
Acetyl-H3K14
Acetyl-H3K18
Acetyl-H3K23
Acetyl-H3K27
H3
15 kDa
Relative protein level of (fold of control)
DMSO
ox-LDL+DMSO
C646
ox-LDL+C646
C
DMSO
Cur
ox-LDL+DMSO
ox-LDL+Cur
IL-6
MCP-1
ChIP (% Input)
NA
BRD2
BRD3
BRD4
P300
H3
D
pcDNA + DMSO
oeBRD4 + DMSO
pcDNA + Cur
oeBRD4 + Cur
Oil Red O
DAPI
Magnification
20X
40X
Relative levels of Oil Red O positive area
ox-LDL
DMSO
Cur
pcDNA
oeBRD4
E
pcDNA
oeBRD4
ox-LDL
DMSO
Cur
DiI-oxldl
DAPI
Relative DIL fluorescence intensity
F
pcDNA
oeBRD4
ox-LDL
DMSO
Cur
LC3
Bodipy
DAPI
G
ox-LDL
Scr
siBRD4
LC3 I
LC3 II
P62
Actin
16 kDa
14 kDa
62 kDa
42 kDa

Figure S3 The histone target of P300 in FCs and the effects of BRD4 overexpression on lipid accumulation in FCs treated with Cur. (A) The bar graph of immunoblot analysis of P300, BRD2, BRD3, BRD4, Actin, Acetyl-H3, and H3 in ox-LDL-treated macrophages combined with Cur treated as in Fig. 2C. (B) Immunoblot analysis of P300 activity in FCs by P300 inhibitor C646. (C) ChIP analysis of the enrichment of P300, BRD2, BRD3, BRD4 and H3 at –1 kb, promoter and +1 kb of *IL-6* and *MCP-1* in Cur-treated FCs. (D–F) The effects of *BRD4* overexpression on lipid accumulation (D), lipid uptake (E) and lipid catabolism (F) in FCs treated with Cur. (G) Immunoblot analysis of the effect of BRD4 on autophagy impairment of FCs by si*BRD4*. Data are expressed as mean ± SEM, $n = 5$. $^{*}P < 0.05$, $^{***}P < 0.001$; $^{\#}P < 0.05$, $^{\#\#\#}P < 0.001$.

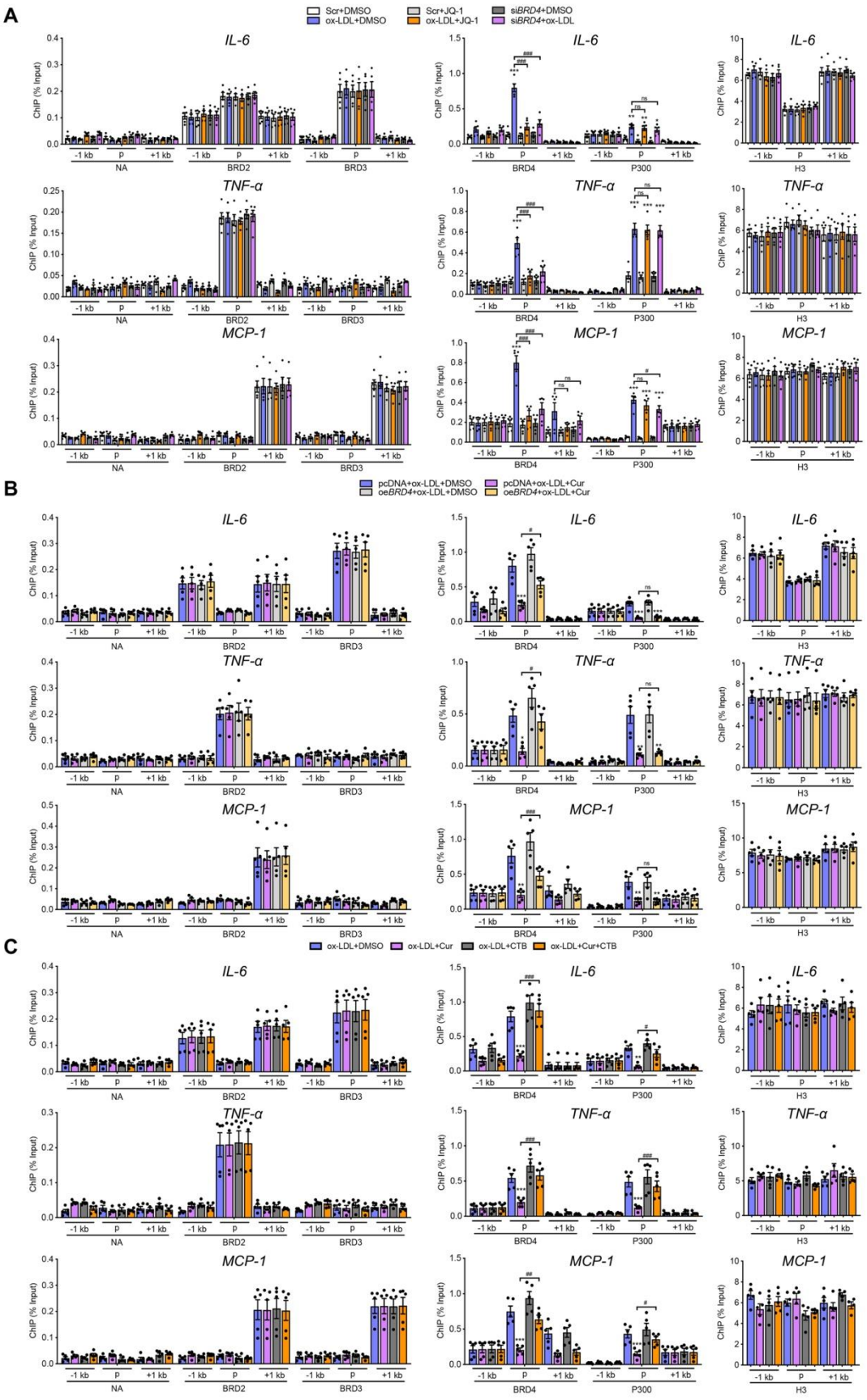
A
Scr+DMSO
ox-LDL+DMSO
Scr+JQ-1
ox-LDL+JQ-1
siBRD4+DMSO
siBRD4+ox-LDL
IL-6
TNF-α
MCP-1
ChIP (% Input)
-1 kb
p
+1 kb
NA
BRD2
BRD3
BRD4
P300
H3
B
pcDNA+ox-LDL+DMSO
oeBRD4+ox-LDL+DMSO
pcDNA+ox-LDL+Cur
oeBRD4+ox-LDL+Cur
C
ox-LDL+DMSO
ox-LDL+Cur
ox-LDL+CTB
ox-LDL+Cur+CTB

Figure S4 Epigenetic landscape of P300-BRD4 dependent inflammatory genes in Cur treated FCs. (A) ChIP analysis of the enrichment of P300, BRD2, BRD3, BRD4 and H3 at –1 kb, promoter and +1 kb of *IL-6*, *TNF-α* and *MCP-1* in ox-LDL-treated macrophages combined with JQ-1 or si*BRD4*. (B, C) The enrichment of P300, BRD2, BRD3, BRD4 and H3 at –1 kb, promoter and +1 kb of *IL-6*, *TNF-α* and *MCP-1* in ox-LDL-treated macrophage combined with Cur in the presence of oe*BRD4* (B) or CTB (C) was measured by ChIP. Data are expressed as mean ± SEM, $n = 5$. $^{*}P < 0.05$, $^{**}P < 0.01$, $^{***}P < 0.001$; $^{\#}P < 0.05$, $^{\#\#}P < 0.01$, $^{\#\#\#}P < 0.001$; ns, no significance.

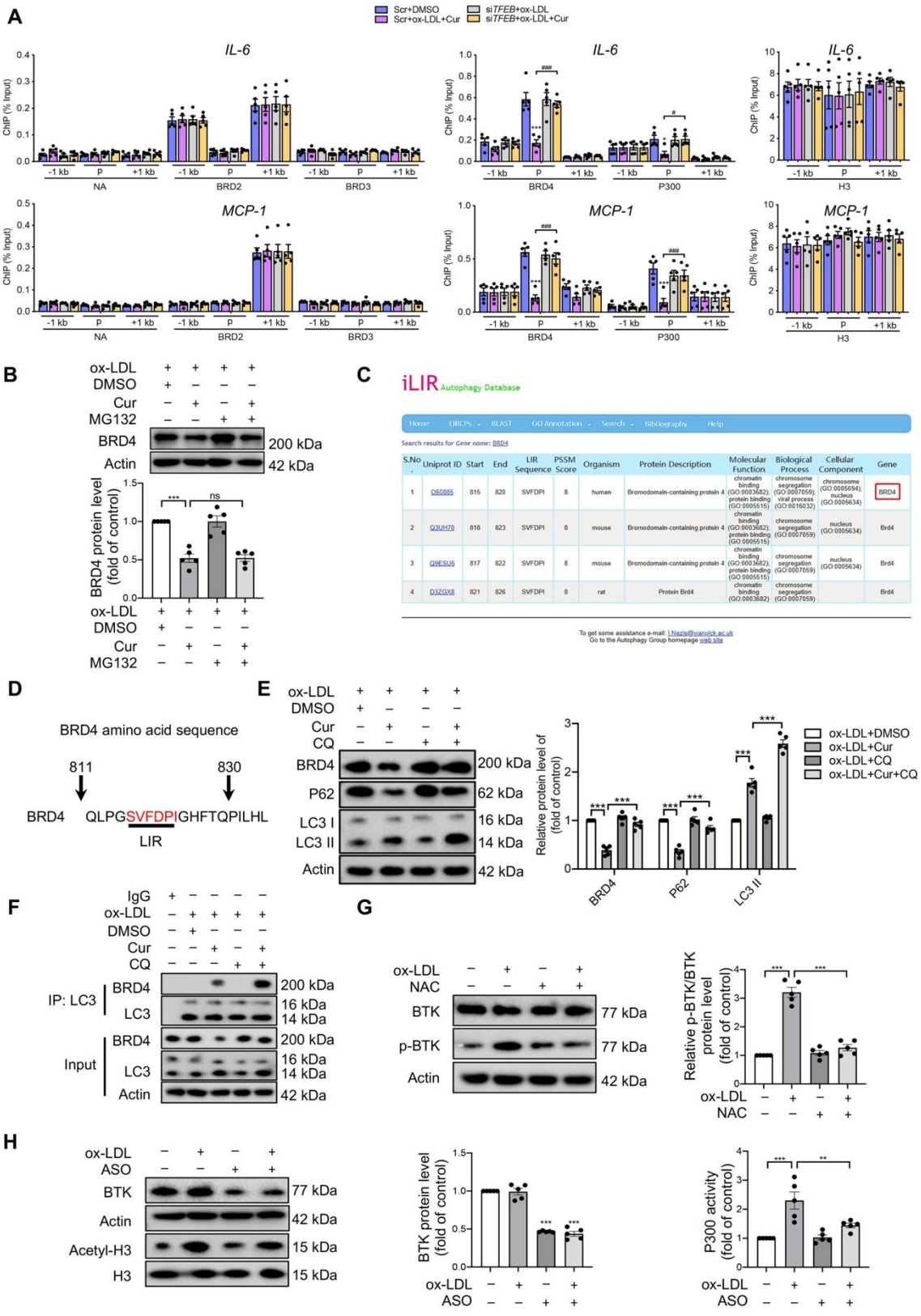
A
Scr+DMSO
Scr+ox-LDL+Cur
siTFEB+ox-LDL
siTFEB+ox-LDL+Cur
IL-6
MCP-1
ChIP (% Input)
-1 kb
P
+1 kb
NA
BRD2
BRD3
BRD4
P300
H3
B
ox-LDL
DMSO
Cur
MG132
BRD4
Actin
200 kDa
42 kDa
BRD4 protein level (fold of control)
ns
C
iLIR Autophagy Database
Home
LIRCPs
BLAST
GO Annotation
Search
Bibliography
Help
Search results for Gene name: BRD4
S.No.
Uniprot ID
Start
End
LIR Sequence
PSSM Score
Organism
Protein Description
Molecular Function
Biological Process
Cellular Component
Gene
1
Q60885
815
820
SVFDPI
8
human
Bromodomain-containing protein 4
chromatin binding (GO:0003682); protein binding (GO:0005515)
chromosome segregation (GO:0007059); viral process (GO:0016032)
chromosome (GO:0005694); nucleus (GO:0005634)
BRD4
2
Q3UH70
818
823
SVFDPI
8
mouse
Bromodomain-containing protein 4
chromatin binding (GO:0003682); protein binding (GO:0005515)
chromosome segregation (GO:0007059)
nucleus (GO:0005634)
Brd4
3
Q9ESU6
817
822
SVFDPI
8
mouse
Bromodomain-containing protein 4
chromatin binding (GO:0003682); protein binding (GO:0005515)
chromosome segregation (GO:0007059)
nucleus (GO:0005634)
Brd4
4
D3ZGX8
821
826
SVFDPI
8
rat
Protein Brd4
chromatin binding (GO:0003682)
chromosome segregation (GO:0007059)
Brd4
To get some assistance e-mail: I.Nezis@warwick.ac.uk
Go to the Autophagy Group homepage web site
D
BRD4 amino acid sequence
811
830
BRD4 QLPGSVFDPIGHFTQPILHL
LIR
E
ox-LDL
DMSO
Cur
CQ
BRD4
P62
LC3 I
LC3 II
Actin
200 kDa
62 kDa
16 kDa
14 kDa
42 kDa
Relative protein level of (fold of control)
ox-LDL+DMSO
ox-LDL+Cur
ox-LDL+CQ
ox-LDL+Cur+CQ
F
IgG
ox-LDL
DMSO
Cur
CQ
IP: LC3
Input
BRD4
LC3
Actin
200 kDa
16 kDa
14 kDa
42 kDa
G
ox-LDL
NAC
BTK
p-BTK
Actin
77 kDa
42 kDa
Relative p-BTK/BTK protein level (fold of control)
H
ox-LDL
ASO
BTK
Actin
Acetyl-H3
H3
77 kDa
42 kDa
15 kDa
BTK protein level (fold of control)
P300 activity (fold of control)

Figure S5 Cur promotes the degradation of BRD4 by autophagy in FCs and the mechanism underlying ROS activating P300 in FCs. (A) ChIP analysis of the enrichment of P300, BRD2, BRD3, BRD4 and H3 at –1 kb from the promoter, at the promoter, and at +1 kb of *IL-6* and *MCP-1* in Cur-treated FCs combined with si*TFEB*. (B) Immunoblot analysis of BRD4 in Cur-treated FCs in the presence of proteosome inhibitor MG132 (10 μmol/L). (C) The iLIR autophagy database shows that BRD4 has LIR motif. (D) The amino acid sequence of BRD4 including LIR motif which is shown in red. (E) Immunoblot analysis of BRD4 in Cur-treated FCs in the presence of autophagic flux inhibitor CQ. (F) Co-immunoprecipitation analysis of the protein interaction between BRD4 and LC3 in Cur-treated FCs in the presence of CQ. (G) Immunoblot analysis of BTK, p-BTK in macrophage treated with ox-LDL in the presence of ROS scavenger NAC. (H) Immunoblot analysis of BTK, Actin, acetyl-H3 and H3 in macrophage treated with ox-LDL in the presence of BTK antisense oligonucleotides (ASO). Data are expressed as mean ± SEM, $n = 5$. $^{*}P < 0.05$, $^{**}P < 0.01$, $^{***}P < 0.001$; $^{\#}P < 0.05$, $^{\#\#\#}P < 0.001$.

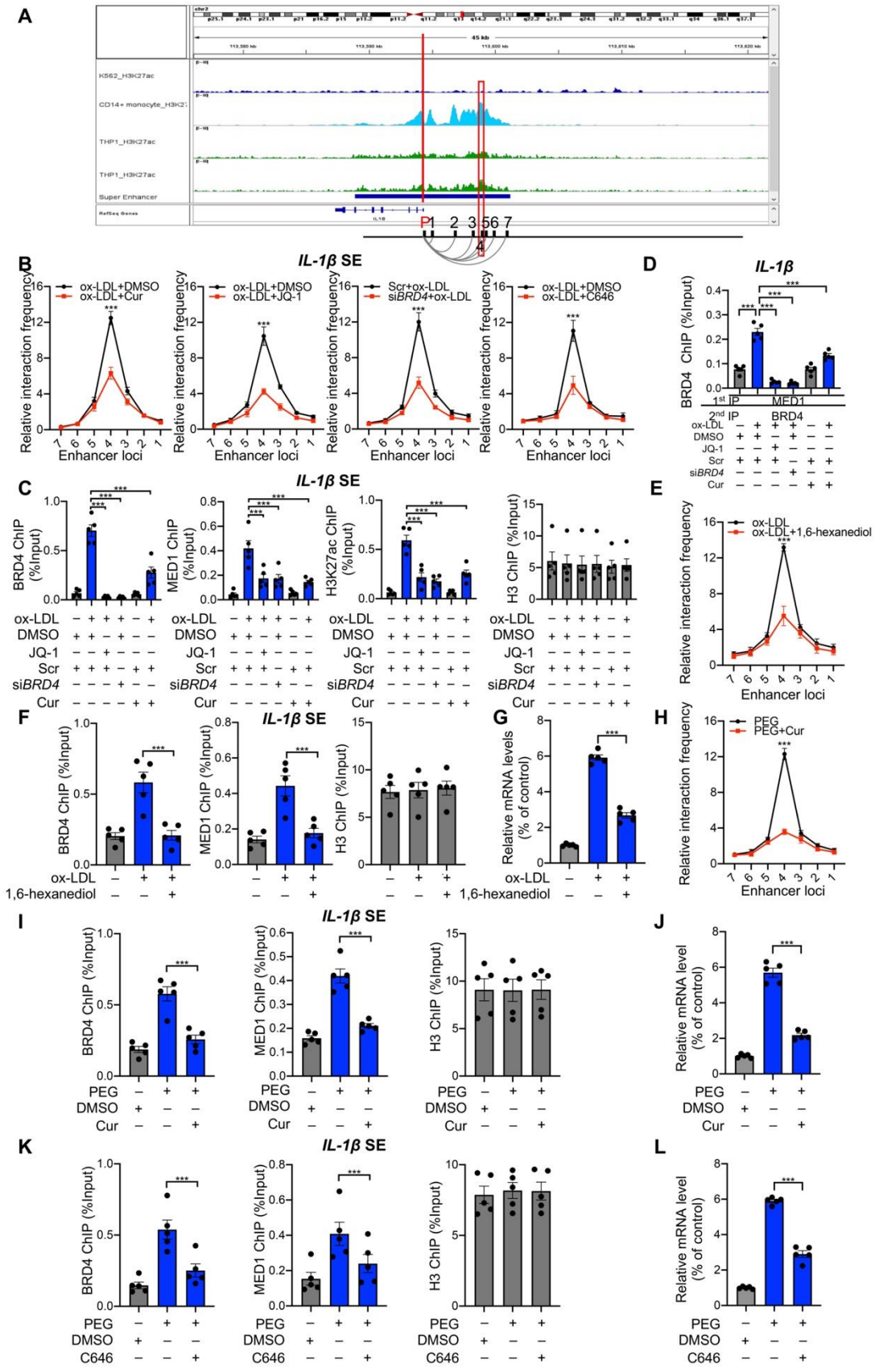
A
K562_H3K27ac
CD14+ monocyte_H3K27
THP1_H3K27ac
THP1_H3K27ac
Super Enhancer
P1 2 3 5 6 7
4
B
IL-1β SE
ox-LDL+DMSO
ox-LDL+Cur
ox-LDL+JQ-1
Scr+ox-LDL
siBRD4+ox-LDL
ox-LDL+C646
Relative interaction frequency
Enhancer loci
C
IL-1β SE
BRD4 ChIP (%Input)
MED1 ChIP (%Input)
H3K27ac ChIP (%Input)
H3 ChIP (%Input)
ox-LDL
DMSO
JQ-1
Scr
siBRD4
Cur
D
IL-1β
BRD4 ChIP (%Input)
1st IP MED1
2nd IP BRD4
ox-LDL
DMSO
JQ-1
Scr
siBRD4
Cur
E
ox-LDL
ox-LDL+1,6-hexanediol
Relative interaction frequency
Enhancer loci
F
IL-1β SE
BRD4 ChIP (%Input)
MED1 ChIP (%Input)
H3 ChIP (%Input)
ox-LDL
1,6-hexanediol
G
Relative mRNA levels (% of control)
ox-LDL
1,6-hexanediol
H
PEG
PEG+Cur
Relative interaction frequency
Enhancer loci
I
IL-1β SE
BRD4 ChIP (%Input)
MED1 ChIP (%Input)
H3 ChIP (%Input)
PEG
DMSO
Cur
J
Relative mRNA level (% of control)
PEG
DMSO
Cur
K
IL-1β SE
BRD4 ChIP (%Input)
MED1 ChIP (%Input)
H3 ChIP (%Input)
PEG
DMSO
C646
L
Relative mRNA level (% of control)
PEG
DMSO
C646

Figure S6 Cur regulates BRD4-dependent super-enhancer (SE) associated with phase separation on *IL-1β*. (A) ChIP-seq peaks (H3K27ac levels) and putative SE location (highlighted by the red box) around *IL-1β*. Cell lines marked with different colors: K562 in blue, CD14-positive monocyte in light blue, THP-1 in green. The putative SE region is marked as the horizontal line in blue. (B) 3C-qPCR analysis of the long-distance interactions between *IL-1β* promoter and seven enhancer loci (the positions of different loci were described as Fig. S6A) in FCs after different treatments (*x*-axis means seven enhancer loci of *IL-1β* promoter). (C) The enrichment of BRD4, MED1, and H3K27ac at the SE region of *IL-1β* in Cur-treated FCs combined with JQ-1, si*BRD4* or Cur was measured by ChIP, as well as H3. (D) Re-ChIP was performed with 1st round pull-down of MED1 antibody and 2nd round pull-down of the BRD4 antibody. (E) 3C-qPCR analysis of the long-distance interactions between *IL-1β* promoter and seven enhancer loci (the positions of different loci were described as Fig. S6A) in FCs treated with 1,6-hexanediol (*x*-axis means seven enhancer loci of *IL-1β* promoter). (F) ChIP analysis of the enrichment of BRD4 and MED1 at the SE region of *IL-1β* in ox-LDL-treated macrophages combined with 3% 1,6-hexanediol, as well as H3. (G) The relative *IL-1β* mRNA level in ox-LDL-treated macrophages combined with 3% 1,6-hexanediol. (H–L) Meanwhile, the macrophages were treated with PEG combined with Cur or P300 inhibitor C646. We detected the long-distance interactions between *IL-1β* promoter and seven enhancer loci in macrophages treated with phase separation crowder PEG and Cur using 3C-qPCR (*x*-axis means seven enhancer loci of *IL-1β* promoter) (H), the enrichment of BRD4 and MED1 at the SE region of *IL-1β* using ChIP (I, K), and the relative *IL-1β* mRNA level using qRT-PCR (J, L). Data are expressed as mean ± SEM, n = 5. $^{***}P < 0.001$.

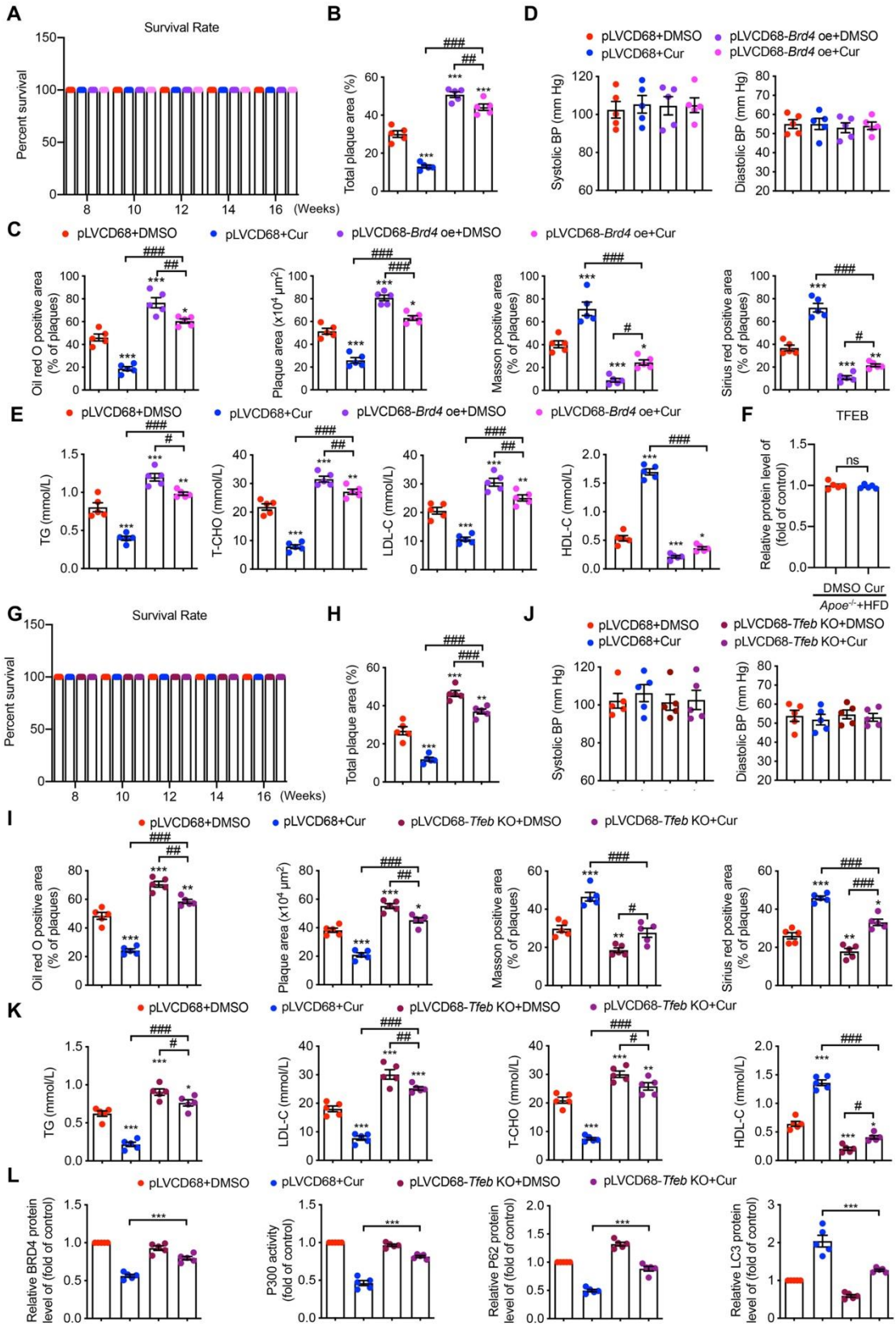
A
Survival Rate
Percent survival
(Weeks)
B
Total plaque area (%)
D
pLVCD68+DMSO
pLVCD68+Cur
pLVCD68-Brd4 oe+DMSO
pLVCD68-Brd4 oe+Cur
Systolic BP (mm Hg)
Diastolic BP (mm Hg)
C
Oil red O positive area (% of plaques)
Plaque area (x10⁴ μm²)
Masson positive area (% of plaques)
Sirius red positive area (% of plaques)
E
TG (mmol/L)
T-CHO (mmol/L)
LDL-C (mmol/L)
HDL-C (mmol/L)
F
TFEB
Relative protein level of (fold of control)
ns
DMSO Cur
Apoe-/-+HFD
G
Survival Rate
Percent survival
(Weeks)
H
Total plaque area (%)
J
pLVCD68+DMSO
pLVCD68+Cur
pLVCD68-Tfeb KO+DMSO
pLVCD68-Tfeb KO+Cur
Systolic BP (mm Hg)
Diastolic BP (mm Hg)
I
Oil red O positive area (% of plaques)
Plaque area (x10⁴ μm²)
Masson positive area (% of plaques)
Sirius red positive area (% of plaques)
K
TG (mmol/L)
LDL-C (mmol/L)
T-CHO (mmol/L)
HDL-C (mmol/L)
L
Relative BRD4 protein level of (fold of control)
P300 activity (fold of control)
Relative P62 protein level of (fold of control)
Relative LC3 protein level of (fold of control)

Figure S7 The statistical graphs of the results in Fig. 7. (A) The survival rate of *Apoe*$^{-/-}$ mice with or without the transplantation of the pLVCD68-*Brd4* overexpression (*Brd4* oe) transduced bone marrow cells (BMCs) combined with Cur. (B) The statistical graph of total plaque area in *Apoe*$^{-/-}$ mice treated as in Fig. 7C. (C) The statistical graph of Oil red O, hematoxylin and eosin, Sirius red and Masson's trichrome staining of the cross-section of the aorta from *Apoe*$^{-/-}$ mice treated as in Fig. 7D. (D) The blood pressure of *Apoe*$^{-/-}$ mice treated as in Fig 7C. (E) The plasma lipids of *Apoe*$^{-/-}$ mice treated as in Fig. 7C. (F) The bar graph of immunoblot analysis of TFEB in *Apoe*$^{-/-}$ mice fed with a HFD and treated with Cur treated as in Fig. 7F. (G) The survival rate of *Apoe*$^{-/-}$ mice with or without the transplantation of the pLVCD68-*Tfeb* knockout (*Tfeb* KO) transduced BMCs combined with Cur. (H) The statistical graph of total plaque area in *Apoe*$^{-/-}$ mice treated as in Fig. 7H. (I) The statistical graph of Oil red O, hematoxylin and eosin, Masson's trichrome and Sirius red staining of the cross-section of the aorta from *Apoe*$^{-/-}$ mice treated as in Fig. 7H. (J) The blood pressure of *Apoe*$^{-/-}$ mice treated as in Fig. 7H. (K) The plasma lipids of *Apoe*$^{-/-}$ mice treated as in Fig. 7H. (L) The bar graph of immunoblot analysis of LC3 II, P62, BRD4, and P300 activity in aortas treated as in Fig. 7L. Data are expressed as mean ± SEM, $n = 5$. $^{*}P < 0.05$, $^{**}P < 0.01$, $^{***}P < 0.001$; $^{\#}P < 0.05$, $^{\#\#}P < 0.01$, $^{\#\#\#}P < 0.001$.